The Development of Reduced Diffusion Following Bevacizumab Therapy Identifies Regions of Recurrent Disease in Patients with High-grade Glioma

Ramon F. Barajas Jr, MD,
Department of Radiology, Neuroradiology Section, Oregon Health & Science University, L340, 3181 S.W. Sam Jackson Park Rd. Portland, OR 97239

Nicholas A. Butowski, MD,
Department of Neurological Oncology, University of California, San Francisco, California

Joanna J. Phillips, MD, PhD,
Department of Pathology, University of California, Box 0628 Bldg 350 Parnassus Ave, Room 307, San Francisco, CA 94143

Manish K. Aghi, MD, PhD,
Department of Neurological Surgery, University of California, San Francisco, California

Mitchel S. Berger, MD,
Department of Neurological Surgery, University of California, San Francisco, California

Susan M. Chang, MD, and
Department of Neurological Oncology, University of California, San Francisco, California

Soonmee Cha, MD
Department of Radiology and Biomedical Imaging, Neuroradiology Section, University of California, Box 0628 Bldg 350 Parnassus Ave, Room 307, San Francisco, CA 94143

Department of Neurological Surgery, University of California, San Francisco, California

Abstract

Rationale and Objectives—The treatment of glioma with bevacizumab results in decreased enhancement, making it challenging to diagnose tumor recurrence. Therefore, the primary aim of this retrospective study was to determine if the underlying biological processes occurring within regions of recurrent glioblastoma in patients undergoing bevacizumab therapy influence morphologic and diffusion-weighted magnetic resonance (MR) imaging characteristics.

Materials and Methods—In this Health Insurance Portability and Accountability Act–compliant and institutional review board–approved study, 26 patients treated with bevacizumab for high-grade glioma underwent lesion-wide apparent diffusion coefficient analysis before therapy and at the time of clinical/radiological progression, allowing for stratification by the presence or absence of reduced diffusion. Lesions with reduced diffusion were classified into "block" or "salt & pepper" phenotypes. Eight of the 26 patients underwent image-guided tissue sampling at the

Address correspondence to: S.C. Soonmee.Cha@uucsf.edu.

time of suspected disease recurrence allowing for direct biological correlation. Clinical, histologic, and MR imaging differences between diffusion groups were assessed using a two-sample Welch *t* test.

Results—All patients had histologic evidence of recurrent disease with or without a background of treatment effect. Sixty-two percent of the cohort had developed reduced diffusion at clinical progression following bevacizumab. Image-guided tissue sampling demonstrated that treatment effect was not observed within regions of reduced diffusion. Recurrent tumor intermixed with treatment effect was more likely to be observed within the "salt & pepper" phenotype when compared to "block" phenotype.

Conclusions—Following bevacizumab therapy, recurrent glioblastoma can manifest as nonenhancing regions characterized by reduced diffusion. Histologically, these MR imaging characteristics correlate with aggressive biological features of disease recurrence.

Keywords

Glioblastoma; bevacizumab; magnetic resonance imaging; apparent diffusion coefficient

INTRODUCTION

High-grade glioma is the malignant form of primary glial neoplasms; the presence of which forebodes poor prognosis. Vascular endothelial growth factor, a hypoxia-regulated gene, is a powerful mediator of tumor progression via its role in tumor angiogenesis and vascular hyperplasia. Bevacizumab, a nonselective monoclonal antibody (mAb) for vascular endothelial growth factor, is clinically used for its antiangiogenic properties in patients with recurrent high-grade glioma.

Currently, the post-therapeutic radiological diagnosis of highgrade glioma recurrence is, in part, characterized by progressive contrast enhancement on serial magnetic resonance (MR) imaging. The presence of contrast enhancement is predicated on the expression of leaky microvasculature. The antiangiogenic effects of bevacizumab histologically causes pseudonormalization of the tumor microvasculature that is biologically manifested as reduced vascular permeability, reduced interstitial pressure, and diminished contrast-enhancing volume on MR imaging. As a result, it can be clinically challenging, in the setting of concurrent bevacizumab administration, to determine whether increasing T2 hyperintensity within a region of diminishing contrast enhancement is a hallmark of tumor response to therapy or the development of nonenhancing recurrent tumor.

Because morphologic MR imaging sequences (T2, axial fluid-attenuated inversion recovery [FLAIR], and T1 post contrast) may fail to accurately determine the true extent of tumor burden in this patient population, some investigators have used diffusion-weighted MR imaging to ascertain additional clinical information that can better prognosticate tumor progression (1–4). Diffusion-weighted imaging (DWI) is an MR imaging technique that measures the diffusion rate of unbound extracellular water molecules. Apparent diffusion coefficient (ADC) is derived from DWI technique and allows for the quantification of diffusivity within tissues. DWI is a widely used clinical MR sequence that holds promise in

the noninvasive assessment of tumor cellularity and hypoxia (5–9). Early investigations into DWI have demonstrated that hypoxia-induced cytotoxic cellular edema and densely packed proliferative tumor cells with a high nuclear-to-cytoplasmic ratio can contribute to the reduction of unbound extracellular water molecular motion that is quantified as decreased ADC values when compared to normal brain.

Previous investigators have noted the presence of reduced diffusion associated with bevacizumab therapy in patients with high-grade glioma; however, tissue sampling of these lesions have yielded mixed findings (1,2). Some reports suggest that the presence of reduced diffusion following bevacizumab therapy is due to hypoxic conditions with no histologic evidence of tumor recurrence. Others report densely cellular recurrent tumor in lesions with reduced diffusion.

Therefore, the primary aim of this retrospective study was to determine if the underlying biological processes occurring within regions of recurrent glioblastoma in patients undergoing bevacizumab therapy influence morphologic and diffusion-weighted MR imaging characteristics. We hypothesized that the development of reduced diffusion following bevacizumab administration would be associated with regions of recurrent tumor that is biologically manifested by elevated cellular proliferative indices.

MATERIALS AND METHODS

Patient Population

Twenty-six adult patients (13 men, 13 women; mean age 52.6 ± 9.8 years; Table 1) referred to our institution's neurologic oncology service for management of histologically confirmed recurrent high-grade glioma were investigated in this retrospective, Health Insurance Portability and Accountability Act–compliant, institutional review board– and committee on human research–approved study. All patients underwent bevacizumab therapy that consisted of 10 mg every other week intravenous infusions. Baseline, concurrent, and follow-up MR imaging examinations were performed throughout the course of therapy. All patients subsequently underwent surgical sampling of clinically/radiologically suspected second episode of disease recurrence concurrent with or following bevacizumab therapy.

MR Imaging Protocol

MR imaging data were obtained on a 1.5T clinical scanner (Signa Horizon, GE Healthcare, Milwaukee, WI) every 4–6 months unless otherwise clinically indicated by disease status. Morphologic sequences included T1 contrast-enhanced, FLAIR, and axial DWI echo-planar imaging (b-value, 1000 s/mm^2).

Morphologic MR Imaging Characterization

MR imaging examinations were blindly analyzed. All MR imaging time points (242 examinations in total for the cohort) between the start of bevacizumab therapy and subsequent surgical diagnosis of disease recurrence were reviewed. Morphologic MR imaging characteristics included lesion anatomic location, presence of contrast enhancement within the cortex and/or subventricular zone, predominant pattern T2 hyperintensity

(edematous, hyperintensity spares cortex; infiltrative, hyperintensity involves cortex), and degree of mass effect (none; mild, midline shift less than 2mm; moderate, midline shift grater than 2 mm, severe, trans-tentorial, uncal, or falcine herniation).

Diffusion-weighted MR Imaging Analysis

Postprocessing of DWI data was performed using commercially available software (FuncTool, GE Healthcare). Morphologic and diffusion images were co-registered, allowing for the production of ADC maps. For each transaxial plane, a region of interest (ROI) was manually defined around the entire region of T2 FLAIR hyperintensity, region of contrast enhancement, and standardized 50 mm^2 contralateral normal-appearing white matter. Areas of central necrosis were excluded from analysis. Minimum, mean, and maximum ADC measurements were obtained within ROIs defining the tumor volume for each patient. Lesion ADC values were standardized to normal-appearing white matter producing relative ADC (rADC) measurements.

The presence of reduced diffusion was defined as lesionwide T2 ADC_{min} <480 ($rADC_{min}$ 0.72) or ADC_{mean} <1003 ($rADC_{min}$ 1.23), which is based on our prior experience in the diagnosis of nonenhancing glioma (5). The pattern of reduced diffusion, when present following bevacizumab therapy, was classified as either "block" or "salt & pepper" phenotypes. "Block" phenotype reduced diffusion was defined by the presence of T2 FLAIR hyperintensity that exhibited a single geographical region of homogenously reduced diffusion without the presence of interspersed regions of T2 FLAIR hyperintense tissue that did not exhibit reduced diffusion (Fig 1). "Salt & pepper" phenotype reduced diffusion was defined by the presence of multiple small foci of reduced diffusion (less than 5 mm^2) within a single region interspersed within regions of T2 FLAIR hyperintense tissue that did not exhibit reduced diffusion (Fig 2). All patients within this cohort demonstrated a single geographic region of reduced diffusion corresponding to one of the two observed phenotypes.

MR Image-guided Biopsy Collection and Processing

All 26 patients underwent surgical tissue sampling following bevacizumab therapy to histologically diagnose the etiology of clinical/radiographic disease progression. MR image-guided tissue sampling was performed on eight of the patients in this cohort and this yielded 24 tissue specimens (5). Tissue sampling was performed on regions of T2 hyperintensity with mean ADC values less than 1300 using image-guided stereotactic neurosurgical techniques.

Tissue specimens were sectioned and stained with hematoxylin and eosin (H&E) stain or mAb, allowing for the histopathologic analysis of biological features of recurrent glioma (overall tumor cellularity, cellular proliferation, necrosis, hypoxia, microvascular density, and microvascular morphology). Microvasculature morphology (factor VIII mAb; delicate morphology, simple vascular hyperplasia morphology, or complex vascular hyperplasia morphology), cellular hypoxia (CA-9), and microvasculature density were scored on a four-tier scale (0, no contribution; 1, minimal; 2, moderate; 3, extensive). Overall tumor cellularity and necrosis were similarly scored using H&E-stained sections. Cellular

proliferation index was determined based on Ki-67 mAb as previously described (5). Tissue specimens were classified as recurrent tumor or treatment effect based on the degree of viable tumor and necrosis within the sample.

Statistical Analysis

The patient cohort was stratified by the presence or the absence of reduced diffusion at the time of radiographic disease progression. Differences between MR imaging and histopathologic metrics were assessed by a two-sample Welch t test. Correlation analysis between ADC values and histopathologic measurements was performed using linear regression. Logistic regression was used to test for an association between diffusion phenotype and the presence of treatment effect following bevacizumab therapy. Sensitivity and specificity was determined using standard binary classification test and receiver operating characteristic curve analysis. A P value <0.05 was considered statistically significant.

RESULTS

Patient Population

All patients had an initial histologic diagnosis of high-grade glioma (glioblastoma, $n = 23$; anaplastic oligodendroglioma, $n = 1$; anaplastic oligoastrocytoma, $n = 2$). On initial diagnosis of disease, all patients received surgical and radiotherapy in combination with temozolomide proceeded by adjuvant temozolomide. Following this initial therapeutic regimen, all patients were diagnosed with recurrent/progressive disease based on increasing T2 FLAIR and contrast enhancing volume and/or worsening neurologic status. All patients underwent surgical and/or medical therapy on diagnosis of recurrent disease that included tissue sampling of the enhancing component providing the pathologic diagnosis of recurrent/ progressive glioblastoma before the initiation of bevacizumab. Subsequent medical therapy included bevacizumab alone or concurrent with irinotecan, carboplatin, and/or temozolomide (Table 1). The median duration of bevacizumab therapy was 4.5 ± 3.4 months (range, 2.25–16 months). One patient was maintained on dexamethasone during bevacizumab therapy. None of the other patients concurrently received corticosteroids during bevacizumab therapy.

All 26 patients had histologically confirmed recurrent glioblastoma with or without treatment concurrent with or subsequent to bevacizumab therapy. The median time from starting bevacizumab therapy to the second diagnosis of recurrent disease for the entire cohort was 5.8 ± 3.4 months (range, 2.5–17.25). Seventy-three percent of the cohort demonstrated recurrent disease without treatment effect (five of the eight patients who underwent image-guided tissue sampling). Twenty-seven percent of the cohort demonstrated mixed recurrent disease within a background of treatment effect (three of eight patients who underwent image-guided tissue sampling).

Distinct Patterns of Disease Recurrence Following Bevacizumab Therapy Are Stratified by Morphologic and Diffusion-weighted MR Imaging Characteristics

All patients demonstrated regions of contrast enhancement without regions of reduced diffusion on the baseline pre-bevacizumab MR imaging examination. Pre-bevacizumab MR morphologic sequences demonstrated moderate to severe mass effect with predominantly edematous T2 pattern in 93% of patients. Post-bevacizumab morphologic sequences showed predominantly infiltrative T2 FLAIR pattern in 60% of the patient cohort.

Sixteen (62%) of the patients developed regions of reduced diffusion within the T2 FLAIR lesion volume following bevacizumab therapy (mean ± standard deviation; 11 ± 8.1 weeks from initiation of therapy, range 2.5 ± 34.2). Reduced diffusion was not observed outside of regions demonstrating T2 FLAIR prolongation. None of the patients were found to have imaging characteristics suggestive of hemorrhage or other susceptibility artifacts that could account for the presence of artificially decreased ADC values. No statistically significant difference in clinically relevant data was observed between the two groups (Supplementary Table S1).

A significant difference in minimum and mean rADC values within the T2 FLAIR and contrast enhancing volume was observed between the pre-bevacizumab and the disease recurrence imaging time points (Table 2; $P < 0.01$). At the time of disease recurrence, regions of reduced diffusion tended to express an infiltrative T2 pattern (14 of 16 patients with reduced diffusion), whereas edematous T2 pattern predominated within the nonreduced diffusion group (8 of 10 patients without reduced diffusion). Only the reduced diffusion group demonstrated a statistically significant decrease in ADC metrics at the time of disease recurrence when compared to pre-therapeutic imaging (Table 3; $P < 0.03$).

ADC Metrics and Lesion Biological Characteristics Within Regions of Treatment Effect Are Significantly Different From Those Composed of Recurrent Glioblastoma

Eight of the 26 patients with recurrent disease following bevacizumab therapy underwent image-guided tissue sampling, yielding 24 specimens. Eighteen tissue specimens demonstrated evidence of recurrent glioblastoma. The remaining six tissue specimens demonstrated findings most consistent with treatment effect. All patients provided at least one tissue specimen consistent with recurrent disease. All tissue specimens consistent with a histopathologic diagnosis of treatment effect were obtained from regions without reduced diffusion (one enhancing and five nonenhancing). Regions of treatment effect had significantly elevated ADC values and decreased cellular proliferation index when compared to recurrent tumor ($P < 0.05$; Table 4).

Regions of Recurrent Glioblastoma Following Bevacizumab Therapy Characterized by Reduced Diffusion Demonstrate Markedly Different Biological Properties Compared to Regions of Recurrent Tumor without Reduced Diffusion

Fourteen tissue samples demonstrating recurrent disease were obtained from regions of reduced diffusion (seven enhancing and seven nonenhancing). Four tissue specimens demonstrating recurrent disease were obtained from regions without reduced diffusion (all nonenhancing). Cellular proliferation (Ki-67; 19.1 ± 13.4 vs. 1.89 ± 1.76; $P < 0.01$), overall

cellularity (H&E; 2.33 ± 0.62 vs. 1.22 ± 1.01; $P = 0.05$), and vascular hyperplasia (factor VIII; 0.90 ± 0.66 vs. 0.22 ± 0.44; $P < 0.01$) were elevated within regions of reduced diffusion compared to regions without reduced diffusion (Fig 3). The expression of delicate vasculature was observed to be significantly increased in regions without reduced diffusion when compared to regions of reduced diffusion (2.11 ± 1.05 vs. 1.13 ± 1.12; $P = 0.04$). Tissue samples from patients with reduced diffusion demonstrated more tissue necrosis than tissue samples from patients without reduced diffusion (1.33 ± 1.09 vs. 0.62 ± 0.52; $P = 0.02$). Sixteen of the tissue specimens (nine from regions of reduced diffusion) were stained for CA-9; a metric of cellular hypoxia. No significant difference in CA-9 expression was observed between regions of reduced diffusion and regions of nonreduced diffusion (1.81 ± 1.37 vs. 1.87 ± 1.24; $P = 0.91$). Additionally, no significant difference was observed between these biological characteristics when stratified by the presence or the absence of contrast enhancement.

For all 24 tissue samples, a statistically significant inverse correlation was observed between ADC values and cellular proliferation (Ki-67/ADC_{min}, R = -0.58, $P < 0.01$; Ki-67/ADC_{mean}, R = -0.38, $P = 0.05$; Ki-67/ADC_{max}, R = -0.48, $P = 0.02$) and overall cellularity (H&E/ADC_{mean}, R = -0.38, $P = 0.05$; H&E/ADC_{max}, R = -0.48, $P = 0.02$) (Fig 4). Additionally, a statistically significant correlation was observed between rADC values and cellularproliferation (Ki-67/rADCmin, R = -0.44, $P = 0.03$; Ki-67/$rADC_{mean}$, R = -0.40, $P = 0.05$) and overall cellularity (H&E/$rADC_{min}$, R = -0.39, $P = 0.05$; H&E/$rADC_{mean}$, R = -0.54, $P < 0.01$; H&E/$rADC_{max}$, R = -0.60, $P < 0.01$). No correlation was observed between ADC metrics and cellular hypoxia (CA-9) or total vascular expression (factor VIII).

Phenotypic Patterns of Reduced Diffusion Are Associated with Histopathologic Characteristics of Recurrent Disease

Regions of reduced diffusion were classified into two mutually exclusive phenotypes: "block" or "salt & pepper" (Figs 1 and 2). Sixty-three percent of patients with reduced diffusion expressed "salt & pepper" phenotype, whereas 37% expressed "block" phenotype. The histologic finding of mixed recurrent glioblastoma in a background of treatment effect was significantly more likely to be observed with the "salt & pepper" phenotype (odds ratio = 7, 95% confidence interval = 1.04–48.3, $P = 0.03$). No statistically significant difference between the two groups was observed in the time it took to develop reduced diffusion following the initiation of bevacizumab therapy (mean ± standard deviation; "block" phenotype = 10 ± 6.2 weeks vs. "salt & pepper" phenotype = 12.4 ± 11 weeks; $P = 0.57$).

Histologic and MR imaging characterization of regions with reduced diffusion, stratified by phenotype, was also performed. "Block" phenotype reduced diffusion had significantly increased necrosis (1.3 ± 1.1 vs. 0.9 ± 0.9; $P = 0.05$) and simple vascular hyperplasia (1.4 ± 1.2 vs. 0.6 ± 0.5; $P = 0.4$) when compared to "salt & pepper" phenotype. While elevated, no differences in Ki-67, CA-9, overall cellularity, vascular hyperplasia, or delicate vasculature expression were observed between regions of reduced diffusion from the two diffusion phenotypes ($P > 0.07$). "Block" phenotype reduced diffusion demonstrated significantly decreased ADC (mean, 592 ± 167 vs. 793 ± 147, $P = 0.05$; max, 743 ± 276 vs.

$1{,}055 \pm 159$, $P = 0.02$) and rADC (mean, $0.81 \pm .15$ vs. $0.99 \pm .18$, $P = 0.05$; max, $0.78 \pm .21$ vs. $1.11 \pm .34$, $P = 0.03$) values when compared to "salt & pepper" phenotype.

Pre-bevacizumab MR Imaging Characteristics Are Predictive of Reduced Diffusion Development Following Bevacizumab Therapy

Eighty-eight percent of patients who developed regions of reduced diffusion demonstrated lesions with contrast enhancement extending from the cortex to the subventricular zone (Type I; 31%) or cortex alone (Type III; 56%) in the setting of predominantly infiltrative T2 pattern on pre-bevacizumab MR imaging. Conversely, 64% of patients who did not develop regions of reduced diffusion demonstrated contrast enhancement of subventricular zone alone (Type II; 9%) or no enhancement of the cortex or subventricular zone (Type IV; 55%) in the setting of predominantly edematous T2 pattern on pre-bevacizumab MR imaging.

Pre-bevacizumab contrast enhancing and T2 FLAIR ADC metrics, obtained up to 3 months before the administration of bevacizumab, were found to be predictive of the subsequent development of visibly discernible reduced diffusion following therapy. Receiver operating characteristic curve analysis identified pre-therapeutic ADC threshold values of 685 for CE ROI and 690 for T2 FLAIR ROI as optimal cutoff values to assess sensitivity and specificity in this cohort. Pre-bevacizumab contrast-enhancing ADC_{min} threshold value of 685 yielded 94% sensitivity and 70% specificity for the development of reduced diffusion following bevacizumab therapy (rADC = 1.12; sensitivity 81%, specificity 70%). Pre-therapeutic T2 FLAIR ADC_{min} threshold value of 690 yielded 86% sensitivity and 50% specificity for the development of reduced diffusion following bevacizumab therapy (rADC = 1.04; sensitivity 75%, specificity 50%).

DISCUSSION

In this retrospective study, we investigated if the underlying biological processes occurring within regions of recurrent glioblastoma in patients undergoing bevacizumab therapy influences morphologic and diffusion-weighted MR imaging characteristics. We demonstrated that a majority of the cohort developed glioblastoma recurrence characterized by infiltrative T2 FLAIR prolongation that was associated with decreased ADC metrics within both enhancing and nonenhancing regions. The histologic finding of mixed recurrent glioblastoma in a background of treatment effect was significantly more likely to be observed with the salt & pepper reduced diffusion phenotype. MR image-guided tissue sampling demonstrated that none of the regions of treatment effect were located within areas of reduced diffusion. Cellular proliferation was significantly increased in regions of recurrent tumor with reduced diffusion. Finally, the development of recurrent disease characterized by reduced diffusion could be predicted with some accuracy through the use of minimum ADC cutoff values. Taken together, these findings provide evidence that a cohort of patients treated with bevacizumab develop regions of glioblastoma recurrence characterized by aggressive biological features that can be delineated by MR imaging. The results of our study can be extrapolated to suggest that tissue sampling of heterogeneously nonenhancing reduced diffusion lesions following bevacizumab therapy should be localized to regions with decreased ADC metrics as these regions are most likely to demonstrate

histologic evidence of recurrent disease, thus reducing the risk of sampling error from within a heterogeneous lesion.

The results of this study have immediate clinical implications for the management of patients currently being treated with antiangiogenic therapy. Most clinical studies investigating the effects of bevacizumab have defined tumor response to therapy based on standardized imaging response criteria, such as RECIST or MacDonald criteria, which are based on measurement of enhancing tumor (10–12). Recent studies have indicated that recurrent glioblastoma disease burden is grossly underestimated by the use of contrast-enhancing volume because it does not account for nonenhancing infiltrative tumor (13,14). The recognition that significant limitations exist in addressing only the tumor's enhancing component when evaluating for progression of disease has led the RANO working group to propose an updated response assessment criteria for high-grade gliomas (15). It is now understood that in patients treated with antiangiogenic therapies, the absence of enhancement is nonspecific in the setting of enlarging T2 FLAIR hyperintensity. Current RANO criteria recommended that enlarging areas of mass like T2 hyperintensity should be considered as evidence of tumor progression. However, current RANO criteria do not account for the development of reduced diffusion following antiangiogenic therapy. Our study provides direct histologic evidence that the development of nonenhancing infiltrative T2 FLAIR prolongation associated with reduced diffusion represents recurrent disease following antiangiogenic therapy.

Previous investigators have noted the presence of reduced diffusion associated with the administration of bevacizumab therapy (16). Rieger et al., in their case series of 18 patients with high-grade glioma treated with bevacizumab, noted that 13 patients developed regions of reduced diffusion. Unguided tissue sampling of one patient demonstrated increased histopathologic measurements of hypoxia-inducible factor 1 alpha subunit, suggesting the presence of hypoxic conditions with no histologic evidence of tumor recurrence or increased tumor cellularity (1). Conversely, Gerstner et al. reported a single patient who developed regions of reduced diffusion concurrent with the administration of bevacizumab (2). Unguided tissue sampling of the tumor demonstrated densely cellular recurrent tumor. From these studies, it was unclear whether tissue specimens were obtained from regions of reduced diffusion or surrounding T2 FLAIR prolongation; in either case, the resulting limited histologic analysis showed markedly different results from tumors with similar MR imaging characteristics.

The results of our study provide an in vivo biological basis for the presence of reduced diffusion within enhancing and nonenhancing regions in recurrent glioblastoma with and without mixed treatment effect following bevacizumab therapy. Diffusivity of unbound extracellular water molecules, as demonstrated by MR DWI, has been demonstrated to become reduced via the decrease of extracellular space resulting from highly cellular tumor with elevated nuclear-to-cytoplasmic ratio and/or in the presence of cellular swelling such as seen in cytotoxic edema in the setting of hypoxic cellular conditions (5–9). In our study, histologic analysis of tissue samples obtained from regions of recurrent tumor characterized by reduced diffusion demonstrated increased tumor mitotic activity, necrosis, and increased factor VIII measurements irrespective of diffusion phenotype or the presence of

enhancement. Elevated mitotic activity was not observed within regions of treatment effect or recurrent tumor not characterized by reduced diffusion. Additionally, we observed no significant difference in the expression of cellular hypoxia (CA-9) between tissue samples of recurrent tumor obtained from regions of reduced diffusion and those from regions of nonreduced diffusion. The lack of correlation between cellular hypoxia expression and ADC metrics implies that the underlying biological factor contributing to the MR imaging manifestation of reduced diffusion for this entire patient cohort is the presence of tumor with increased mitotic activity. The lack of hypoxia expression within recurrent high-grade glioma following bevacizumab has also been suggested by prior investigations using 18F-fluoromisonidazole positron emission tomography/MR imaging (17).

In our study, the development of reduced diffusion was characterized by one of two imaging phenotypes that could be distinctly identified: "block" or "salt & pepper." To our knowledge, phenotype classification of regions of reduced diffusion in patients with recurrent glioblastoma following the administration of bevacizumab has not been previously proposed. This classification is relevant as our study suggests both biological and clinical implications. The observation that mixed recurrent tumor in a background of treatment effect was more likely to be observed in patients demonstrating the salt & pepper phenotype suggests the clinical relevance of this classification system. In this clinical scenario, it would be prudent for tissue sampling to occur in regions of reduced diffusion as this could reduce the likelihood of false-negative results.

Our study has several important limitations. First, the small sample size and lack of subjects without disease recurrence caution against overinterpretation of our findings. Future investigations should attempt to identify the MR imaging characteristics within a cohort of patients who develop histologically proven pseudo-progression without any evidence of recurrent tumor following bevacizumab therapy. Second, qualitative diffusion analysis was performed at two time points (immediately before bevacizumab therapy and at the time of disease progression), which precluded analysis of the predictive role of serial ADC measurements during bevacizumab treatment (18,19). Third, the observed decrease in ADC values cannot be entirely attributed to bevacizumab therapy because some patients did concurrently receive other chemotherapies. Future prospective studies will have to control for these confounding variables. Finally, the small sample size precluded a survival analysis to adjudicate whether the observed MR imaging characteristics were associated with a worse clinical outcome in this patient cohort.

CONCLUSION

Our study demonstrates that the biological processes occurring within regions of recurrent glioblastoma treated with bevacizumab therapy influences MR imaging. Specifically, a cohort of patients treated with bevacizumab develop regions of glioblastoma recurrence characterized by aggressive biological features manifested as invasive T2 FLAIR prolongation and reduced diffusion.

Supplementary Material

Refer to Web version on PubMed Central for supplementary material.

Acknowledgments

APPENDIX. SUPPLEMENTARY MATERIAL

Supplementary data to this article can be found online at doi:10.1016/j.acra.2016.04.004.

Abbreviations and Acronyms

ADC	apparent diffusion coefficient
DWI	diffusion-weighted imaging
FLAIR	axial fluid-attenuated inversion recovery
H&E	hematoxylin and eosin
mAb	monoclonal antibody
MR	magnetic resonance
rADC	relative apparent diffusion coefficient
ROI	region of interest

References

1. Rieger J, Bähr O, Müller K, et al. Bevacizumab-induced diffusion-restricted lesions in malignant glioma patients. J Neurooncol. 2010; 99:49–56. [PubMed: 20035366]

2. Gerstner ER, Frosch MP, Batchelor TT. Diffusion magnetic resonance imaging detects pathologically confirmed, nonenhancing tumor progression in a patient with recurrent glioblastoma receiving bevacizumab. J Clin Oncol. 2010; 28:e91–e93. [PubMed: 19933906]

3. Jain R, Scarpace LM, Ellika S, et al. Imaging response criteria for recurrent gliomas treated with bevacizumab: role of diffusion weighted imaging as an imaging biomarker. J Neurooncol. 2010; 96:423–431. [PubMed: 19859666]

4. Pope WB, Kim HJ, Huo J, et al. Recurrent glioblastoma multiforme: ADC histogram analysis predicts response to bevacizumab treatment. Radiology. 2009; 252:182–189. [PubMed: 19561256]

5. Barajas RF Jr, Hodgson JG, Chang JS, et al. Glioblastoma multiforme regional genetic and cellular expression patterns: influence on anatomic and physiologic MR imaging. Radiology. 2010; 254:564–576. DOI: 10.1148/radiol.09090663 [PubMed: 20093527]

6. Le Bihan D, Turner R, Douek P, et al. Diffusion MR imaging: clinical applications. AJR Am J Roentgenol. 1992; 159:591–599. [PubMed: 1503032]

7. Rowley HA, Grant PE, Roberts TP. Diffusion MR imaging: theory and applications. Neuroimaging Clin N Am. 1999; 9:343–361. [PubMed: 10318719]

8. Le Bihan D, Breton E, Lallemand D, et al. MR imaging of intravoxel incoherent motions: application to diffusion and perfusion in neurologic disorders. Radiology. 1986; 161:401–407. [PubMed: 3763909]

9. Guo AC, Cummings TJ, Dash RC, et al. Lymphomas and high-grade astrocytomas: comparison of water diffusibility and histologic characteristics. Radiology. 2002; 224:177–183. [PubMed: 12091680]

10. Therasse P, Arbuck SG, Eisenhauer EA, et al. New guidelines to evaluate the response to treatment in solid tumors: European Organization for Research and Treatment of Cancer, National Cancer Institute of the United States, National Cancer Institute of Canada. J Natl Cancer Inst. 2000; 92:205–216.

11. Macdonald DR, Cascino TL, Schold SC, et al. Response criteria for phase II studies of malignant glioma. J Clin Oncol. 1990; 8:1277–1280. [PubMed: 2358840]

12. Norden AD, Young GS, Setayesh K, et al. Bevacizumab for recurrent malignant gliomas; efficacy, toxicity, and patterns of recurrence. Neurology. 2008; 70:779–787. [PubMed: 18316689]

13. Iwamoto FM, Abrey LE, Beal K, et al. Patterns of relapse and prognosis after bevacizumab failure in recurrent glioblastoma. Neurology. 2009; 73:1200–1206. [PubMed: 19822869]

14. Verhoeff J, Tellingen O, Claes A, et al. Concerns about anti-angiogenic treatment in patients with glioblastoma multiforme. BMC Cancer. 2009; 9:444. [PubMed: 20015387]

15. Wen PY, Macdonald DR, Reardon DA, et al. Updated response assessment criteria for high-grade gliomas: response assessment in neurooncology working group. J Clin Oncol. 2010; 28:1963–1972. [PubMed: 20231676]

16. Gupta A, Young RJ, Karimi S, et al. Isolated diffusion restriction precedes the development of enhancing tumor in a subset of patients with glioblastoma. AJNR Am J Neuroradiol. 2011; 32:1301–1306. [PubMed: 21596805]

17. Barajas RF Jr, Pampaloni MH, Clarke JL, et al. Assessing biological response to bevacizumab using 18F-Fluoromisonidazole PET/MR imaging in a patient with recurrent anaplastic astrocytoma. Case Rep Radiol. 2015; 2015:731361. [PubMed: 25793136]

18. Pope WB, Qiao XJ, Kim HJ, et al. Apparent diffusion coefficient histogram analysis stratifies progression-free and overall survival in patients with recurrent GBM treated with bevacizumab: a multi-center study. J Neurooncol. 2012; 108:491–498. [PubMed: 22426926]

19. Ellingson BM, Cloughesy TF, Lai A, et al. Quantification of edema reduction using differential quantitative T2 (DQT2) relaxometry mapping in recurrent glioblastoma treated with bevacizumab. J Neurooncol. 2012; 106:111–119. [PubMed: 21706273]
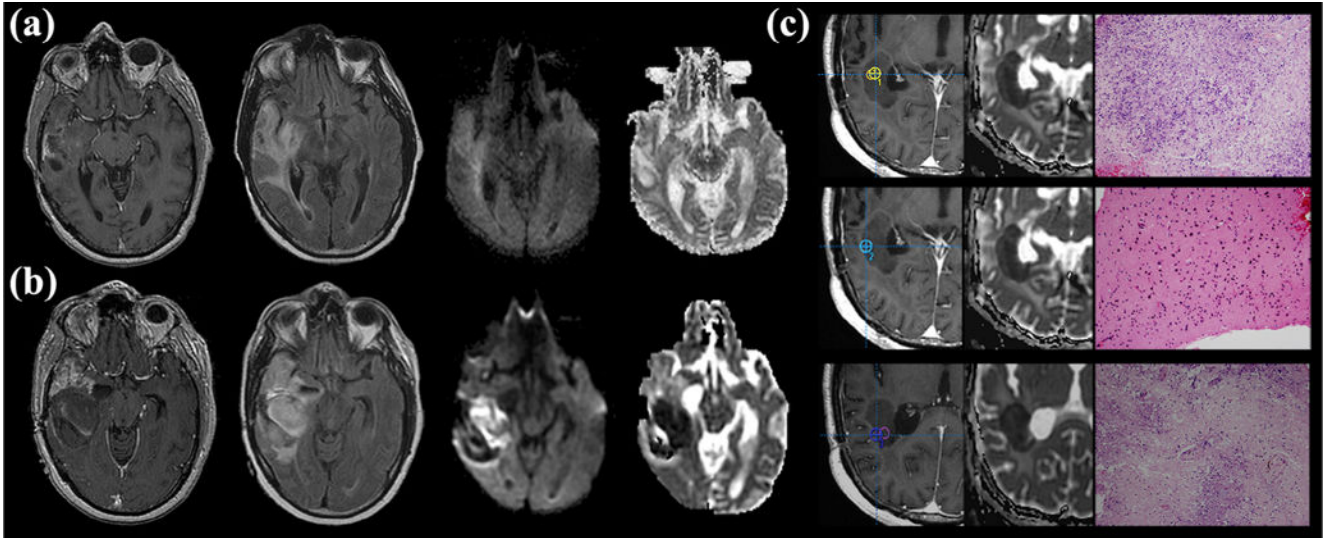
Figure 1.
Development of block phenotype reduced diffusion in a 50-year-old man following 3 months of bevacizumab therapy. **(a)** Pre-therapeutic T1-weighted contrast-enhanced (*left*), axial fluid-attenuated inversion recovery (FLAIR) (*center left*), diffusion-weighted image (*center right*), and apparent diffusion coefficient (ADC) map (*right*) show no indication of reduced diffusion. **(b)** Post-therapeutic magnetic resonance (MR) imaging demonstrates interval development of mass like infiltrative minimally enhancing T2 hyperintensity and block phenotype reduced diffusion involving the right temporal lobe (lesion average T2 ADCmin = 350, ADCmean = 967, $rADC_{min}$ = 0.49, and rADCmean = 1.1). Pre-contrast T1-weighted images (*not shown*) did not demonstrate T1-shortening/blood products that would account for artificially reduced diffusion. Robust contrast enhancement predominately involving the anterior temporal lobe is not associated with reduced diffusion. **(c)** Image-guided tissue sampling of reduced diffusion lesion (*left*; T1 postcontrast sampling site, *center*; ADC map, *right*; hematoxylin and eosin [H&E]) showed heterogeneous highly cellular recurrent tumor with some samples demonstrating increased cellular necrosis (H&E stain, 10× Mmagnification; top and bottom samples; greater than 50%) when compared to regions demonstrating densely cellular tumor recurrence without necrosis (*middle sample*). Markedly elevated measures of cellular proliferation, vascular hyperplasia, and necrosis were also observed within regions of reduced diffusion when compared to regions without reduced diffusion (*not shown*).
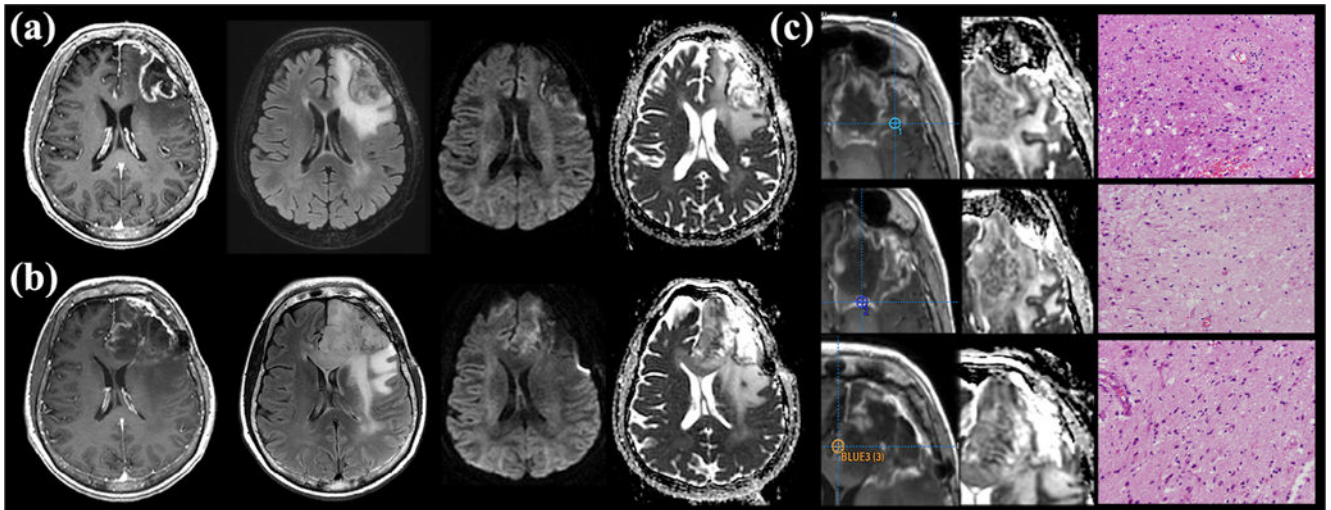
Figure 2.
Development of salt & pepper phenotype reduced diffusion in a 57-year-old woman following 2 months of bevacizumab therapy. **(a)** Pre-therapeutic T1-weighted contrast-enhanced (*left*), axial fluid-attenuated inversion recovery (FLAIR) (*center left*), diffusion-weighted image (*center right*), and apparent diffusion coefficient (ADC) map (*right*) show no indication of reduced diffusion. Note the region of artificially reduced diffusion along the medial aspect of the resection cavity due to blood products that subsequently resolved. **(b)** Post-bevacizumab magnetic resonance (MR) imaging demonstrates interval development of mass like infiltrative T2 hyperintensity involving the frontal lobe with extension into the cingulate gyrus and genu of the corpus callosum associated with salt & pepper phenotype reduced diffusion (lesion average T2 ADCmin = 665, ADCmean = 1082, $rADC_{min}$ = 0.95, and rADCmean = 1.3). Minimal contrast enhancement involves the region of reduced diffusion. **(c)** Image-guided tissue sampling of the lesion (*left*; T1 post contrast sampling site, *center*; ADC map, *right*; hematoxylin and eosin [H&E]) showed heterogeneous regions of recurrent tumor and treatment-related changes (H&E stain; 200× magnification). Tissue sample #3 (bottom), corresponding to a region of reduced diffusion, demonstrated infiltrating recurrent tumor with minimal necrosis. Tissue samples #1 and #2 (*top and middle*) corresponded to regions without reduced diffusion. Tissue sample #1 demonstrated infiltrating recurrent tumor margin with minimal necrosis. Tissue sample #2 demonstrated extensive necrosis without evidence of recurrent tumor most consistent with treatment effect.
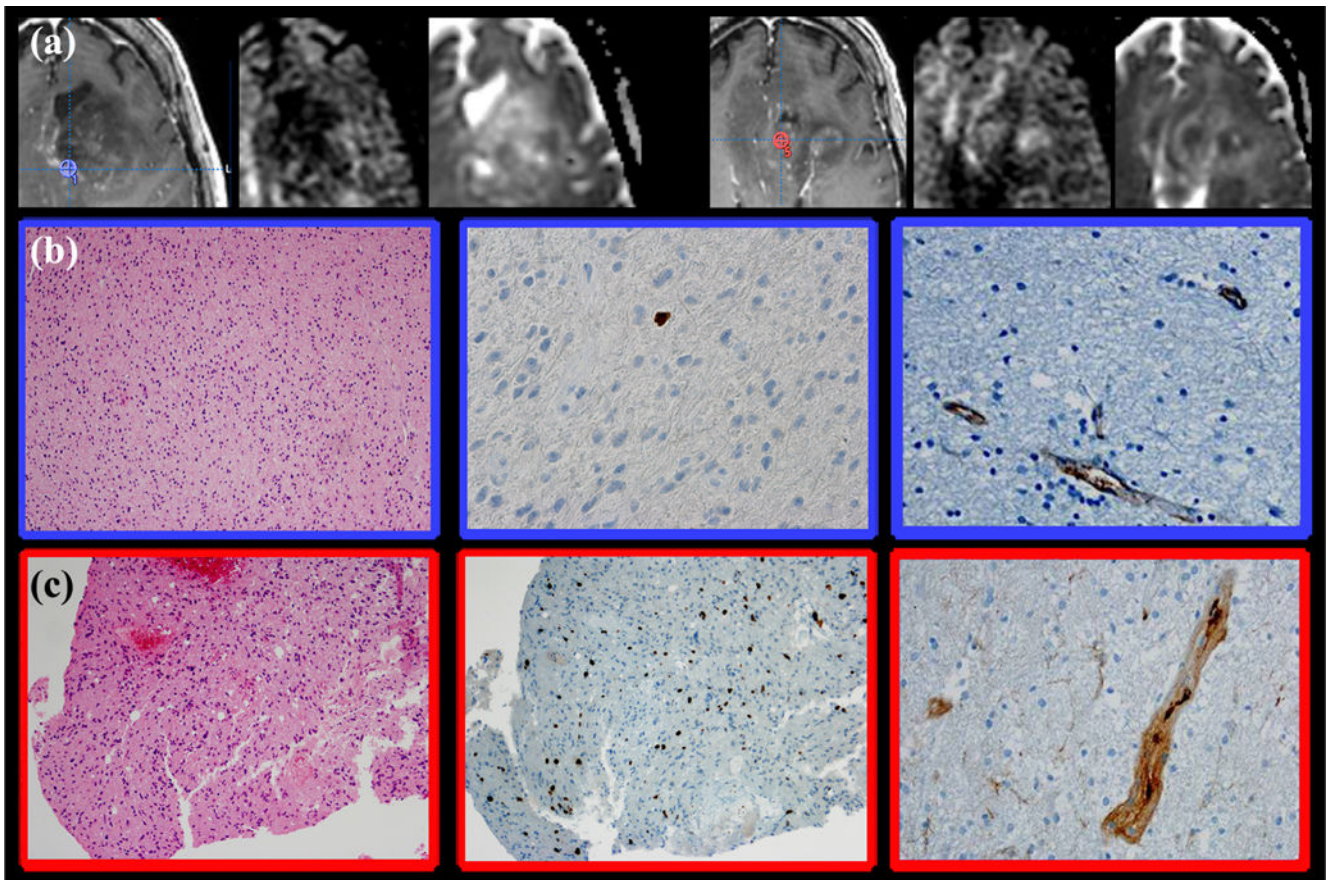
Figure 3.
Histopathologic correlation of recurrent glioblastoma tissue samples obtained from regions with and without reduced diffusion using image-guided stereotactic neurosurgical techniques in a patient demonstrating salt & pepper phenotype following bevacizumab therapy. **(a)** Intraoperative tissue sampling site superimposed on a post-therapeutic T1-weighted contrast-enhanced image, diffusion-weighted image, and apparent diffusion coefficient (ADC) map demonstrates mass like infiltrative T2 hyperintensity involving the left frontal lobe associated with salt & pepper phenotype reduced diffusion and minimal contrast enhancement. Tissue sampling site from region without reduced diffusion (*left*) demonstrated ADC_{min} of 842 and ADC_{mean} of 951. Tissue sampling site from region with reduced diffusion demonstrated ADC_{min} of 485 and ADC_{mean} of 646 (*right*). **(b)** Tissue samples obtained from region of recurrent tumor without reduced diffusion (*blue region of interest [ROI]*) demonstrated infiltrating cellular tumor (*left*; H&E stain 200× magnification), cellular proliferation of 1% (*middle*; Ki-67), with minimal vascular hyperplasia (*right*; factor VIII = delicate vascular appearance). **(c)** Tissue samples obtained from region of recurrent tumor with reduced diffusion (*red ROI*) demonstrated infiltrating cellular tumor (*left*; H&E stain 10× magnification) with elevated cellular proliferation (*middle*; Ki-67 = 11%), and predominantly simple vascular hyperplasia (*right*; factor VIII). No significant necrosis was observed within either tissue specimens. (Color version of figure is available online.)
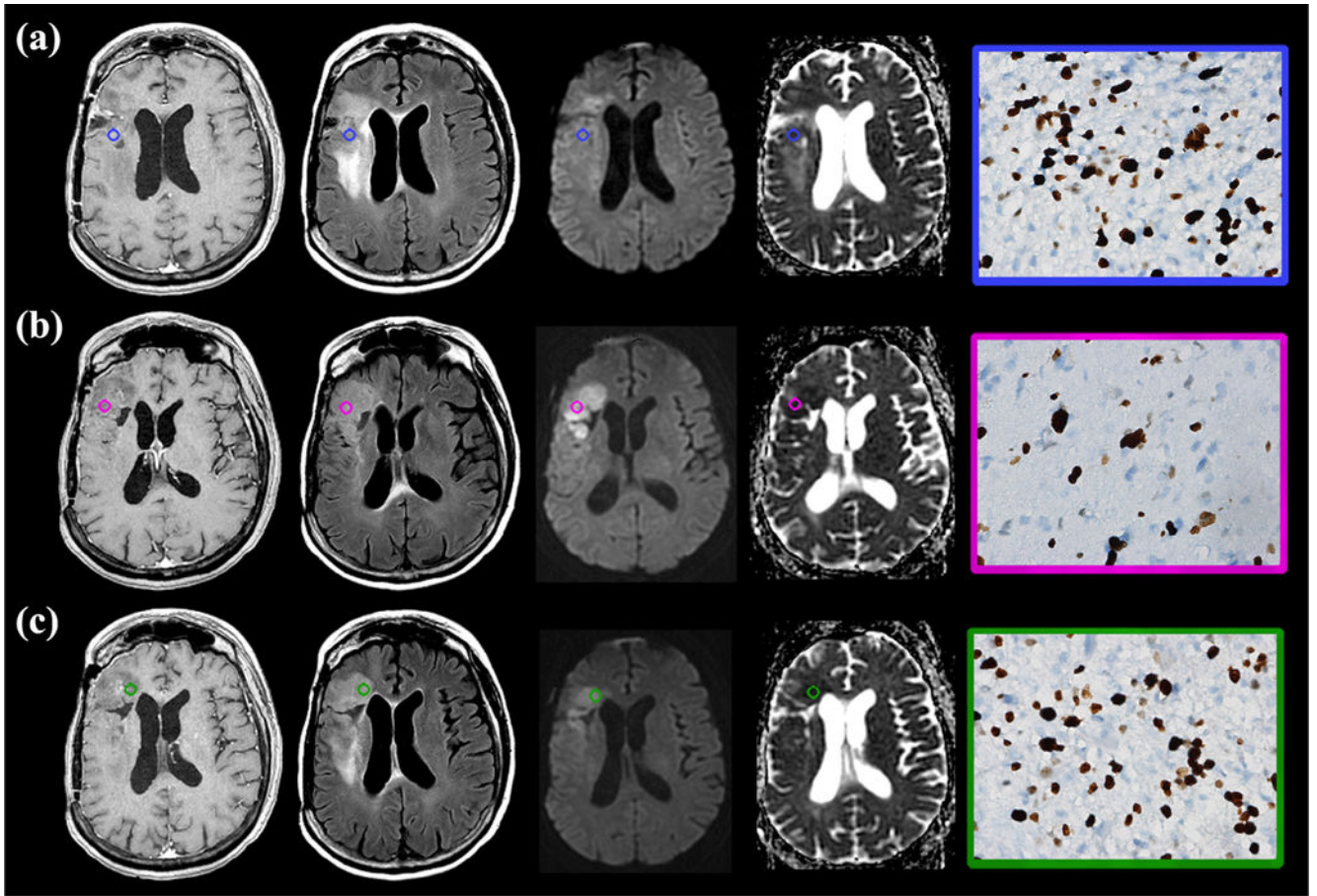
Figure 4.
Recurrent glioblastoma following bevacizumab therapy with block phenotype reduced diffusion demonstrates elevated cellular proliferation. **(a–c)** Post-therapeutic T1-weighted contrast enhanced (*left*), axial fluid-attenuated inversion recovery (FLAIR) (*center left*), diffusion-weighted image (*center right*), and apparent diffusion coefficient (ADC) map (*right*) demonstrate mass like infiltrative T2 hyperintensity involving the frontal operculum associated with block phenotype reduced diffusion and minimal contrast enhancement. All tissue sampling sites were obtained within regions of reduced diffusion (ADC$_{min}$ A–C = 315, 336, and 246; ADC$_{mean}$ A–C = 365, 406, and 287; color circle region of interest [ROI]). Immunohistochemical analysis demonstrated markedly elevated cellular proliferation (Ki-67 A–C = 32%, 26%, and 29%, brown-stained cells; right column) irrespective of the presence (biopsy site C) or absence (biopsy sites A and B) of contrast enhancement. Additionally, elevated necrosis (H&E, less than 50%; not shown) was observed. (Color version of figure is available online.)

TABLE 1

Clinical and Qualitative MR Imaging Measurements

Patient Number	Initial Dx	Age	Image-guided Tissue Sample	KPS	Pathology	Group	Concurrent Therapies	Location	SVZ	Post Tx T2 Pattern	DWI Phenotype
1	GBM	53	N	90	Recurrent	Rd	CPT, Carbo	F	3	I	S
2	GBM	50	N	80	Recurrent	Rd	CPT	F	3	I	S
3	GBM	50	N	90	Mixed	Rd	Carbo	F	3	E	S
4	GBM	64	N	80	Mixed	Rd	None	O	3	I	S
5	GBM	50	N	90	Recurrent	Rd	TMZ	T	1	I	B
6	GBM	63	N	90	Mixed	Rd	CPT	P	3	E	S
7	GBM	42	N	70	Recurrent	Rd	CPT	T	4	I	B
8	GBM	62	N	70	Recurrent	Rd	CPT	P	1	I	S
9	GBM	64	Y	70	Recurrent	Rd	None	P	1	I	B
10	AO	54	Y	90	Mixed	Rd	CPT	F	3	I	B
11	AOA	47	Y	90	Mixed	Rd	CPT	P	2	I	S
12	GBM	38	Y	90	Recurrent	Rd	TMZ	F	3	I	S
13	AO	56	Y	70	Recurrent	Rd	None	P	3	I	B
14	GBM	57	Y	80	Mixed	Rd	TMZ	F	3	I	S
15	GBM	62	Y	80	Recurrent	Rd	None	P	1	I	S
16	GBM	51	Y	90	Recurrent	Rd	None	P	1	I	B
17	GBM	52	N	90	Recurrent	NRd	Carbo	T	3	E	None
18	GBM	58	N	80	Recurrent	NRd	CPT	P	2	E	None
19	GBM	64	N	80	Recurrent	NRd	CPT	T	3	E	None
20	GBM	27	N	90	Recurrent	NRd	TMZ	P	4	E	None
21	GBM	35	N	90	Recurrent	NRd	TMZ	T	4	I	None
22	GBM	47	N	90	Recurrent	NRd	CPT	P	4	I	None
23	GBM	68	N	90	Mixed	NRd	None	P	4	E	None
24	GBM	58	N	90	Recurrent	NRd	None	F	1	E	None
25	GBM	56	N	80	Recurrent	NRd	None	P	4	E	None
26	GBM	47	N	90	Recurrent	NRd	CPT	F	4	E	None

AO, anaplastic oligodendroglioma; AOA, anaplastic oligoastrocytoma; B, block; CPT, irinotecan, carbo, Paraplatin; DWI phenotype, reduced diffusion-weighted imaging phenotype; E, edematous; F, frontal; GBM, glioblastoma; I, infiltrative; Initial Dx, initial histologic diagnosis; KPS, Karnofsky Performance Scale Index (obtained before initiation of bevacizumab); Mixed, recurrent glioblastoma within background of treatment change/effect; NRd, nonreduced diffusion; O, occipital; P, parietal; Pathology, pathologic diagnosis at time of recurrence following Avastin; Post Tx T2 Pattern, post-

bevacizumab therapy T2 pattern; Rd, reduced diffusion; Recurrent, recurrent glioblastoma; S, salt & pepper; SVZ, subventricular zone; T, temporal; Tissue Sample, underwent image-guided tissue sampling, Yes or No; TMZ, temozolomide; Type 1, enhancement contacting cortex and subventricular zone; Type 2, enhancement contacting subventricular zone alone; Type 3, enhancement contacting cortex alone; Type 4, no enhancement of the cortex or subventricular zone.

TABLE 2

Comparison of Pre- and Post-therapeutic Diffusion-weighted Imaging for All Patients

	T2 Area (cm^2)	T2 $rADC_{min}$	T2 $rADC_{mean}$	T2 $rADC_{max}$	CE Area (cm^2)	CE $rADC_{min}$	CE $rADC_{mean}$	CE $rADC_{max}$
PreTx	13.4(12.2)	0.99 (0.15)	1.66 (0.34)	2.12 (0.40)	2.36 (2.94)	1.12 (0.33)	1.51 (0.23)	1.88 (0.43)
PostTx	17.7 (9.8)	0.71 (0.21)	1.30 (0.18)	2.02 (0.54)	3.82 (7.08)	0.82 (0.23)	1.20 (0.33)	1.61 (0.55)
*P*value	0.16	0.01	0.01	0.41	0.34	0.01	0.01	0.05

CE, contrast enhancing region of interest; Mean (standard deviation), T2, T2 FLAIR hyperintensity region of interest; PostTx, following bevacizumab administration; PreTx, before bevacizumab administration.

TABLE 3

Comparison Diffusion-weighted Imaging Values for Reduced Diffusion Group

	T2 Area	T2	T2	T2R	CE Area	CE	CE	CE
	(cm²)	rADC_{min}	rADC_{mean}	rADC_{max}	(cm²)	rADC_{min}	rADC_{mean}	rADC_{max}
PreTx	17.3 (13.0)	0.95 (0.15)	1.71 (0.41)	2.06 (0.35)	3.25 (3.43)	1.01 (0.18)	1.46 (0.23)	1.81 (0.35)
PostTx	20.5 (9.91)	0.58 (0.13)	1.210.13)	1.88 (0.59)	4.49 (8.69)	0.69 (0.17)	1.05 (0.13)	1.35 (0.59)
P value	0.44	0.01	0.01	0.30	0.60	0.01	0.01	0.01

CE, contrast enhancing region of interest; Max, maximum value; Mean, average value; Mean (standard deviation), T2, T2 FLAIR hyperintensity region of interest; Min, minimum value; PostTx, following bevacizumab administration; PreTx, before bevacizumab administration.

TABLE 4

Comparison of Diffusion-weighted Imaging and Cellular Proliferation Metrics Between Regions with Recurrent Tumor and Treatment Effect

	ADC_{min}	ADC_{mean}	ADC_{max}	$rADC_{min}$	$rADC_{mean}$	$rADC_{max}$	Ki-67
RT	541 (179)	711 (206)	892 (260)	0.96 (0.21)	0.93 (0.23)	0.94 (0.31)	16.3 (13.5)
TE	838 (78)	1154 (110)	1455 (257)	1.36 (0.36)	1.62 (0.35)	1.76 (0.31)	1.7 (1.63)
P value	<0.01	<0.01	<0.01	0.04	<0.01	<0.01	<0.01

ADC, apparent diffusion coefficient; Ki-67, expressed in percentage; rADC, relative apparent diffusion coefficient; RT, recurrent tumor; TE, treatment effect.